Null test for a highly paraboloidal mirror

Taehee Kim, James H. Burge, Yunwoo Lee, and Sungsik Kim

A circular null computer-generated hologram (CGH) was used to test a highly paraboloidal mirror (diameter, 90 mm; *f* number, 0.76). To verify the null CGH test a classic autocollimation test with a flat mirror was performed. Comparing the results, we show that the results of the null CGH test show good agreement with results of the autocollimation test. © 2004 Optical Society of America

OCIS codes: 120.3180, 220.4840, 120.6650.

1. Introduction

In recent years the design of compact optical systems has become increasingly important. The use of highly aspheric surfaces makes it theoretically possible achieve this compactness. But there is a question whether the aspheric surfaces needed can be fabricated, and one cannot fabricate such surfaces unless they can be tested.[1,2]

Aspheric surfaces are tested by use of an interferometric null configuration. The interferometry measures the difference in wave front between a reference surface and test surface. If the test surface has the desired shape, the output of the interferometer will be null.[3]

The null corrector is placed in the interferometer to generate a reference wave front that matches the desired test surface. The application of a lens as a null corrector requires using a complex compound consisting of optical elements. Because each additional lens adds alignment errors and optical fabrication errors that must be controlled, a null lens corrector is generally expensive. But the null computer-generated hologram (CGH) corrector allows aspheric surfaces to be measured easily without use of expensive multiple lenses.[4–6]

Because the final quality of an aspheric surface depends on the accuracy of the null test used to guide its fabrication, verification of the null test is necessary. Agreement between tests when an independent null corrector is used can give strong verification that both are correct.[4]

In this paper, null tests that use two different kinds of null corrector are discussed. A circular null CGH is applied to interferometry for testing a paraboloidal mirror (diameter, 90 mm; *f*-number, 0.76). The results are compared with those measured by a classic autocollimation test. The correlation between the two tests is analyzed.

2. Design of a Null Computer-Generated Hologram

A. Null Computer-Generated Hologram

Optical testing with a circular null CGH is characterized in a double-pass configuration. For simplicity, we consider a single-pass configuration as shown in Fig. 1.

We assume that the perfect wave-front match can be achieved. The phase function of the CGH is derived by use of a geometrical model of rays normal to the aspheric surface. The ray $O'H'$ passing through position $H'(r)$ on the CGH intersects the axis at I. Ray OH passing through center $H(r_0)$ on the CGH is directed toward point I.

Optical path $O'H'I$ is given by

$$O'H'I(r) = O'H' + H'I, \tag{1}$$

$$O'H' = [(H'_x - O'_x)^2 + (H'_y - O'_y)^2 + (H'_z - O'_z)^2]^{1/2}, \tag{2}$$

$$H'I = [(I_x - H'_x)^2 + (I_y - H'_y)^2 + (I_z - H'_z)^2]^{1/2}. \tag{3}$$

T. Kim (th1.kim@samsung.com) and S. Kim are with the Digital Media Research and Development Center, Samsung Electronics Company, Ltd., Suwon City, Kyungki-do 442-742, Korea. J. H. Burge is with the Optical Sciences Center, University of Arizona, Tucson, Arizona 85721. Y. Lee is with the Division of Optical Metrology, Korea Research Institute of Standards and Science, P.O. Box 102 Yuseong, Daejeon 305-600, Korea.

Received 24 October 2003; revised manuscript received 23 March 2004; accepted 29 March 2004.

0003-6935/04/183614-05$15.00/0

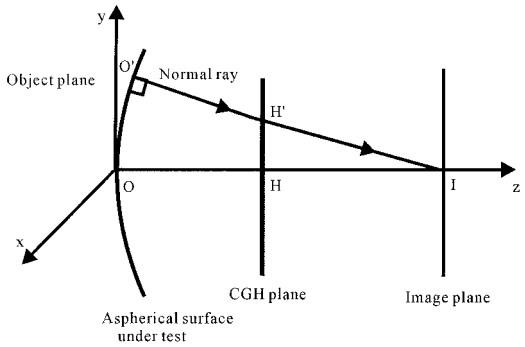

Fig. 1. Geometry for defining a CGH such that it returns the same wave front as a perfect aspheric surface.

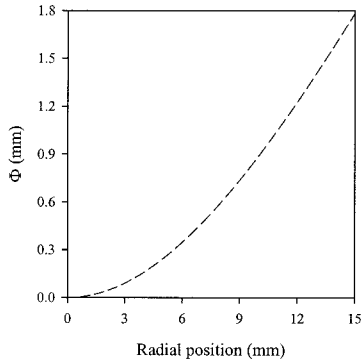

Fig. 3. CGH function calculated at the CGH plane for paraboloid testing.

Optical path *OHI* is given by

$$OHI(r_0) = OH + HI, \tag{4}$$

$$OH = |H_z - O_z|, \tag{5}$$

$$HI = |I_z - H_z|. \tag{6}$$

The CGH function is the path difference between *O′H′I* and *OHI*. Choosing the arbitrary reference point as the center yields the following CGH function across the CGH[3]:

$$\phi(r) = O'H'I(r) - OHI(r_0). \tag{7}$$

Figure 2 shows the layout with prescription of a null CGH test for a 90-mm diameter, 0.76 *f*-number paraboloidal mirror whose parameters are given in Table 1. The CGH function calculated from Eq. (7) by use of the prescription is shown in Fig. 3. The resultant wave-front aberration for first diffraction order is less than a peak-to-valley (P–V) value of 0.001λ at a wavelength of 633 nm.

B. Alignment Computer-Generated Hologram

Misalignment causes errors in test results. To prevent errors and facilitate easy and quick alignment, alignment CGHs are used. We designed the alignment CGH to find the correct CGH position and distance between the CGH and the paraboloid. The design was done as follows.

- Adjustment of CGH position: Assume that a spatial filter is both the object plane and the image plane, as shown in Fig. 4(a). Rays from object point are diffracted onto the CGH and reflected back exactly to the image point.
- Adjustment of distance from the CGH to the paraboloid: Assume that a spatial filter is the object plane and that a vertex plane of the paraboloid is the image plane, as shown in Fig. 4(b). Rays from the

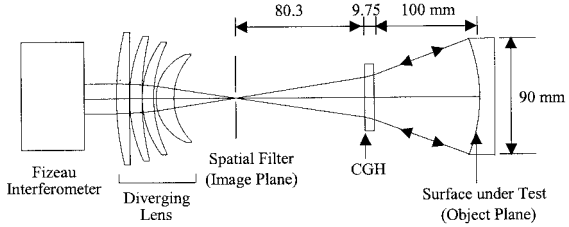

Fig. 2. Layout with prescription of a null CGH test for a paraboloid mirror.

Table 1. Design Data for a Paraboloidal Mirror

Parameter	Value
Radius (mm)	120
Conic constant	−1
Diameter (mm)	110
Clear aperture (mm)	90
f-number	0.76
Material	Fused silica
Maximum sag from vertex plane (mm)	8.4
Maximum sag from best-fit radius (mm)	0.073

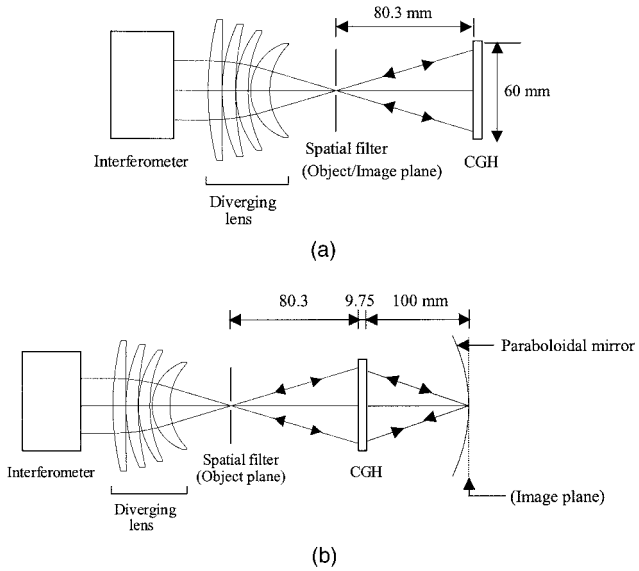

Fig. 4. Layout for design of alignment CGHs: (a) adjustment of CGH position, (b) adjustment of distance from the CGH to the paraboloid.

Table 2. Phase Coefficients of an Alignment CGH

Phase Coefficient	Alignment CGH: Position of CGH	Alignment CGH: Distance from CGH to Paraboloid
C_1	-0.003582557452	-3.333333×10^{-3}
C_2	$0.1023842252 \times 10^{-6}$	$8.333333254 \times 10^{-8}$
C_3	$-0.58487212 \times 10^{-11}$	$-0.41667488 \times 10^{-11}$
C_4	$0.420196916 \times 10^{-15}$	$0.261028598 \times 10^{-15}$
C_5	$-0.3408795 \times 10^{-19}$	$-0.2077156 \times 10^{-19}$
C_6	$0.297683539 \times 10^{-23}$	$0.769386165 \times 10^{-23}$
C_7	$-0.26261844 \times 10^{-27}$	$-0.97568134 \times 10^{-26}$
C_8	$0.178569714 \times 10^{-31}$	$0.884782617 \times 10^{-29}$
C_9		$-0.44655134 \times 10^{-32}$
C_{10}		$0.955991197 \times 10^{-32}$

object point are diffracted onto the CGH and focused on the vertex of the aspheric surface.

For commercially available software a circular CGH function is represented by

$$\phi(r) = \frac{1}{m}\,(C_1 r^2 + C_2 r^4 + C_3 r^6 + \cdots), \qquad (8)$$

where r is the radial distance from the CGH's center and m is the operating diffraction order. C_i is the phase coefficient on the $2i$th power of r, which is adjusted to optimize the system's performance.

We designed the alignment CGHs by using Eq. (8) with the prescription of Fig. 4. The phase coefficients optimized for the third diffraction order are summarized in Table 2. The resultant wave-front aberration was less than 0.001λ P–V at a wavelength of 633 nm.

The CGH structural data obtained by encoding the CGH functions given above are listed in Table 3. Figure 5 shows the main CGH and the alignment CGHs as they were written onto the same fused-silica substrate by a laser writing machine at the Institute of Automation and Electrometry, Novosibirsk, Russia.[7] The CGHs were fabricated based on the process described in Refs. 5 and 8.

The main CGH for a paraboloid is designed to be used as a phase type in the first-order transmission mode. It has a circular aperture with a 31-mm diameter and a 50% duty cycle. It contains 2971 rings; the spacing between adjacent rings in the CGH decreases with increasing ring radius. The smallest ring spacing is 3 μm at the edge of the CGH. It has a gating grove depth of 1 λ. The alignment CGHs consist of segment A1 for adjusting a CGH's position and segment A2 for adjusting the distance from a CGH to the paraboloid. The former CGH is designed to be used as a chrome-on-glass type in third-order reflection mode. The latter is designed to be used as a phase type in the third-order transmission mode.

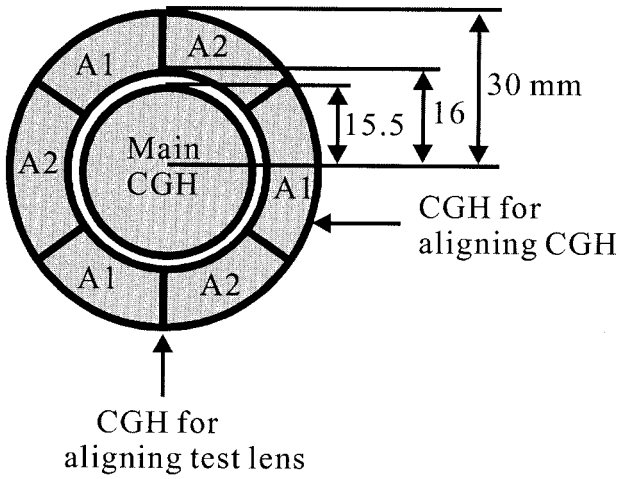

Fig. 5. CGH consisting of a main area for generating the paraboloidal test wave surrounded by six smaller diffractive sectors.

3. Experiments

A. Null Computer-Generated Hologram Test

A null CGH is used with a phase-shifting Fizeau interferometer (wavelength, 632.8 nm) at the Korea Research Institute of Standards and Science (KRISS) for autocollimation testing of paraboloids that have been manufactured by polishing. A schematic of the layout for this test is shown in Fig. 2. Because a

Table 3. CGH Structure Parameters[a]

Parameter[b]	Main CGH	Alignment CGH: CGH Position (A1)	Alignment CGH: Distance from CGH to Paraboloid (A2)
Grating type	Binary phase grating	Binary chrome-on-glass grating	Binary phase grating
Material (chrome)		$n_{\text{chrome}} = 3.6 - i4.4$	
Material (glass)		Fused silica ($n_{\text{glass}} = 1.46$)	
Operating mode	Transmission	Reflection	Transmission
Diffraction order	First	Third	Third
Smallest grating spacing (μm)	3.3	3.3	3.1
Grating groove depth	1λ (2π rad)	Chrome thickness, 100 nm	1λ (2π rad)
Grating duty cycle		50%	

[a] λ = 632.8 nm.
[b] The materials are chrome ($n_{\text{chrome}} = 3.6 - i4.4$) and fused silica ($n_{\text{glass}} = 1.46$). The grating duty cycle is 50%.

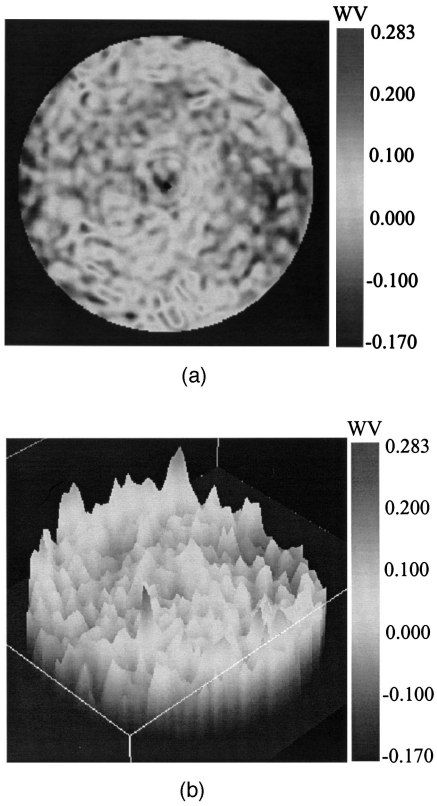

Fig. 6. (a) Two-dimensional and (b) three-dimensional plots of the wave-front phase-difference map. Here and in Figs. 7 and 8, WV means wavelength.

circular CGH generates multiple diffraction orders along the optical axis, a spatial filter is used to block the unwanted orders of diffraction.

To reduce random errors in the measured wave-front phase map we averaged the results of five measurements. To reduce alignment errors during the measurement we removed wave-front tilt and power from the phase map. Low-pass filtering was performed to reduce high-frequency noise. The final phase maps are shown in Fig. 6. The paraboloid has a figure error of 0.31λ P–V and a rms error of 0.04λ. The figure error was calculated from a Zernike polynomial by use of 36 terms of the WYKO vision software.

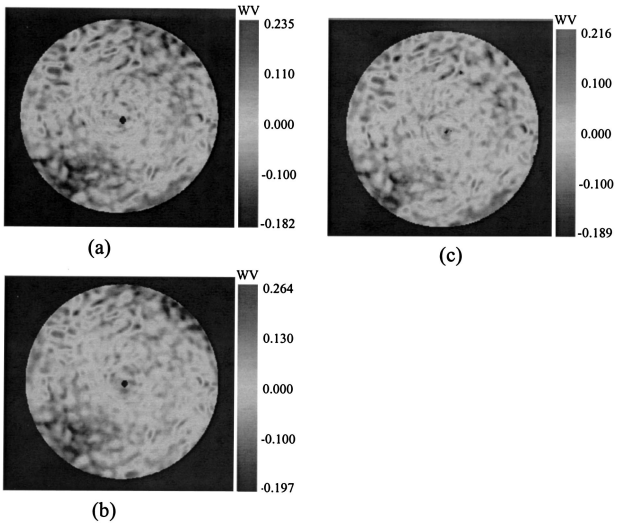

Fig. 7. Wave-front phase-difference map obtained from rotation of the CGH. Rotation angles were (a) 0°, (b) 120°, and (c) 240°.

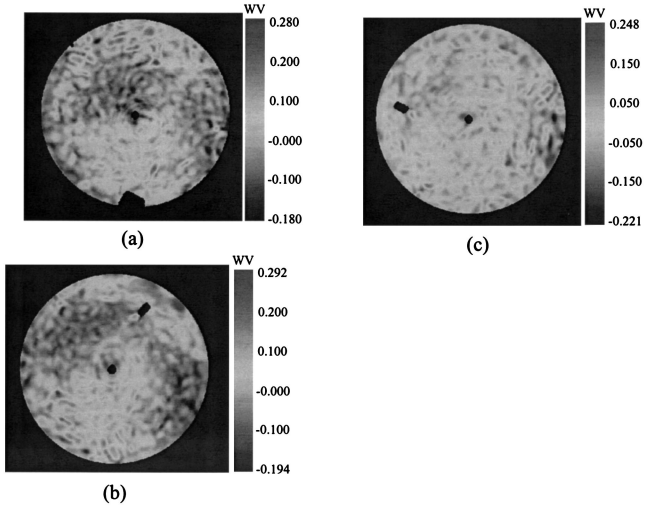

Fig. 8. Wave-front phase-difference map obtained from rotation of the paraboloid. Rotation angles were (a) 0°, (b) 120°, and (c) 240°. The dark shapes near the edges of the circles are fiducial marks that were used for alignment.

Nonaxisymmetric astigmatism errors can be observed in the phase map of Fig. 6. To verify the source of the astigmatism we performed rotation tests. The CGH was rotated three times, in 120° increments, and remeasured. The phase maps derived from three measurements are shown in Fig. 7. Because the astigmatism orientation did not rotate with the CGH, the problem did not lie in the CGH. We measured independently the phase maps by rotating the paraboloidal mirror. The maps that resulted from these measurements are shown in Fig. 8. Because the errors did not rotate with the paraboloid, they did not exist in the paraboloid. On the basis of these observations we estimate that the astigmatism in the phase map came from systematic errors in the measurement.

B. Autocollimation Test

The layout of an autocollimation test with a flat mirror is shown in Fig. 9. An autocollimation test uses

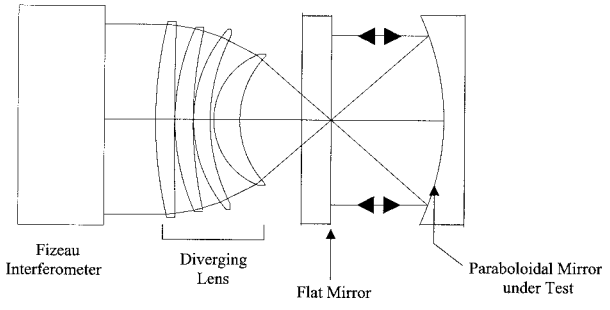

Fig. 9. Autocollimation test for the paraboloid.

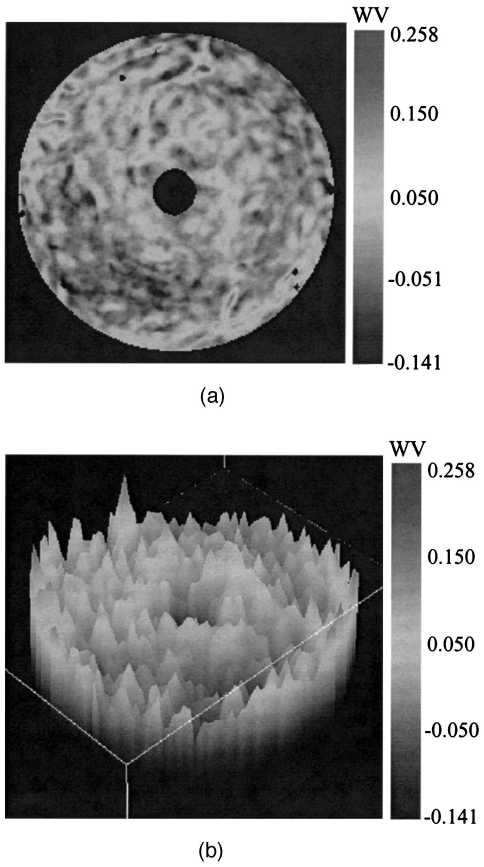

Fig. 10. (a) Two-dimensional and (b) three-dimensional plots of the wave-front phase-difference map.

a point source at the focus of the paraboloid to create collimated light on reflection. A flat mirror reflects this light directly back to the paraboloid, where it reflects to form a point image.

Figure 10 shows the wave-front phase maps obtained from the test. The effects of the flat mirror were not taken into account because the figure error caused by a flat mirror is much smaller than an error on the parabolic surface. A figure error of 0.36λ P–V with a rms error of 0.05λ can be observed.

The test results described above are summarized in Table 4. The wave-front errors that resulted from the autocollimation test were in excellent agreement with the amount measured by use of the same test at the KRISS. The wave-front error measured by the null CGH test matched the autocollimation test result within 0.05λ P–V and a rms error of 0.01λ. Therefore it can be seen that the ability of the null CGH test to quantify the figure error of a parabolic surface accurately is confirmed.

Table 4. Comparison of Null CGH and Autocollimation Tests[a]

	Measured Value		
Wavefront Error	Null CGH Test	Autocollimation Test	Autocollimation Test at KRISS
P–V	0.36λ	0.31λ	0.31λ
rms	0.05λ	0.04λ	0.04λ

[a]λ = 633 nm.

4. Conclusions

In this paper we have studied null tests for a highly paraboloidal mirror (diameter, 90 mm; *f*-number, 0.76). Circular null CGH and alignment CGH designs were discussed, and the measured phase maps and an analysis of the error were given. To verify the results of the null CGH test we performed the classic autocollimation test with a flat mirror. The null CGH results were compared with those of the autocollimation test. The wave-front phase difference between two results was less than 0.05λ P–V. As a result, we could confirm the validity of the null CGH test for paraboloids.

The authors thank A. G. Poleshchuk of the Institute of Automation and Electrometry, Novosibirsk, Russia, for fabricating the CGH.

References

1. J. M. Sassian, "Design of null lens correctors for the testing of astronomical optics," Opt. Eng. **27,** 1051–1056 (1988).
2. S. A. Lerner and J. M. Sassian, "Use of implicitly defined optical surfaces for the design of imaging and illumination systems," Opt. Eng. **39,** 1796–1801 (2000).
3. S. R. Clark, "Optical reference profilometry," Ph.D. dissertation (Optical Sciences Center, University of Arizona, Tucson, Ariz., 2000).
4. J. H. Burge, "Advanced techniques for measuring primary mirrors for astronomical telescopes," Ph.D. dissertation (Optical Sciences Center, University of Arizona, Tucson, Ariz., 1993).
5. Y.-C. Chang, "Diffraction wavefront analysis of computer-generated holograms," Ph.D. dissertation (Optical Sciences Center, University of Arizona, Tucson, Ariz., 1993).
6. J. H. Burge, "Measurement of large convex asphere," in *Optical Telescopes of Today and Tomorrow*, A. L. Ardeberg, ed., Proc. SPIE **2871,** 362–372 (1997).
7. A. G. Poleshchuk, E. G. Churin, V. P. Koronkevich, V. P. Korolkov, A. A. Kharissov, V. V. Cherkashin, V. P. Kiryanov, A. V. Kiryanov, S. A. Kokarev, and A. G. Verhoglyad, "Polar coordinate laser pattern generator for fabrication of diffractive optical elements with arbitrary structure," Appl. Opt. **38,** 1295–1301 (1999).
8. V. V. Cherkashin, A. A. Kharisov, V. P. Korl'kov, V. P. Koronkevich, and A. G. Poleshchuk, "Accuracy potential of circular laser writing of DOEs," in *Optical Information Science and Technology* (*OIST97*): *Computer and Holographic Optics and Image Processing*, A. L. Mikaelian, ed., Proc. SPIE **3348,** 58–68 (1998).